Molecular Origins of the Thermal Transitions and Dynamic Mechanical Relaxations in Perfluorosulfonate Ionomers

Kirt A. Page, Kevin M. Cable, and Robert B. Moore*

Department of Polymer Science, The University of Southern Mississippi, Hattiesburg, Mississippi 39406-0001

Received February 18, 2005; Revised Manuscript Received April 21, 2005

ABSTRACT: The study presented here is a fundamental investigation into the molecular origins of the thermal transitions and dynamic mechanical relaxations of Nafion membranes as studied by DSC, DMA, variable temperature small-angle X-ray scattering (SAXS), and solid-state ^{19}F NMR spectroscopy. While several studies in the literature have attempted to explain the molecular origins of these thermal transitions and mechanical relaxations, the assignments were based primarily on limited DMA results and have at times been contradictory. In DSC traces of Nafion, the low- and high-temperature endotherms are shown to be dependent on thermal history and are now attributed to melting of relatively small and large crystallites, respectively. DSC analysis of Nafion yields information only on the crystalline nature of this ionomer, and neither of the transitions can be assigned to glass transitions. The intensity of the small-angle ionomer peak at ca. $q = 2$ nm^{-1} was monitored as a function of temperature for each alkylammonium neutralized sample. Changes in intensity of the ionomer peak as a function of temperature were shown to correlate well with the α and β relaxations observed in DMA. Variable temperature solid-state ^{19}F NMR techniques were used to investigate the dynamics of the Nafion chains. Spin-diffusion experiments revealed a profound increase in mobility at the onset of the α relaxation. Sideband analysis indicated that the side chain is more mobile than the main chain and that the mobility is greatly affected by the size of the counterion. Molecular level information from this analysis in correlation with SAXS and DMA data supports the assignment of the β relaxation to the genuine T_g of Nafion and the α relaxation to the onset of long-range mobility of chains/side chains via a thermally activated destabilization of the electrostatic network.

Introduction

Perfluorosulfonate ionomers (PFSI's) are copolymers containing runs of tetrafluoroethylene and generally less than 15 mol % of perfluorovinyl ether units that are terminated with a sulfonic acid exchange site. PFSI's have proven to be an interesting class of materials due to their wide applicability in electrochemical processes such as chlor-akali cells,[1] water electrolyzers,[2] batteries, and fuel cells.[3,4] The most widely studied PFSI, and the focus of this investigation, is the PFSI Nafion, which is a product of the Dupont Chemical Co. having the following structure:

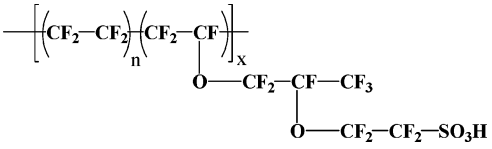

The polar perfluoroether side chains containing the ionic sulfonate groups have been shown to organize into aggregates, thus leading to a nanophase-separated morphology where the ionic domains, termed clusters,[5] are distributed throughout the nonpolar poly(tetrafluoroethylene) (PTFE) matrix. In addition, the runs of tetrafluoroethylene, of sufficient length, are capable of organizing into crystalline domains having unit cell dimensions virtually identical to that of pure PFTE.[6,7] The degree of crystallinity in PFSI's is generally less than ca. 10 wt % in 1100 equivalent weight Nafion (i.e., EW, the grams of dry polymer per equivalent of SO_3^- groups) and has been shown to vary with equivalent weight. The complex, phase-separated morphology, consisting of crystalline and ionic domains, of PFSI's has been the focus of several investigations aimed at characterizing the morphology[5,7−19] and the thermomechanical[20−26] behavior of these materials.

Numerous morphological studies of Nafion have focused on the small-angle X-ray scattering behavior of this unique ionomer.[5,7−19] With electron density differences between the ionic domains and the PTFE matrix, a scattering maximum appears in small-angle X-ray scattering profiles at ca. $q = 1-2$ nm^{-1}, which has been termed the "ionomer peak". In addition, a very low-angle peak or shoulder is often observed at ca. $q = 0.5$ nm^{-1}, which has been attributed to scattering from the locally ordered crystallites composed of relatively long runs of PTFE segments between side chains.[5,8] Several structural models have been proposed in order to explain the origins of the ionomer peak in Nafion;[5,7−19] however, for the purposes of this study, it is only necessary that the ionomer peak be attributed to the existence of ionic aggregates that are distributed throughout the matrix with some degree of spatial heterogeneity. With respect to thermal and mechanical properties, these ionic domains are generally accepted to constitute the electrostatic network within PFSI's (i.e., physical cross-links that can inhibit segmental mobility).

Previous differential scanning calorimetry (DSC) studies of dry neutralized PFSI materials have revealed two endothermic peaks below 300 °C in the initial heating scan of these materials.[7,20,21,24,27] These endothermic events observed in DSC have been correlated to data obtained from dynamic mechanical analysis of these materials. For example, the two thermal transi-

* To whom all correspondence should be addressed: e-mail rbmoore@usm.edu; Ph 601-266-4480; Fax 601-266-5504.

10.1021/ma0503559 CCC: $30.25
Published on Web 06/30/2005

tions (endothermic events) have been noted to occur at temperatures that are comparable to two distinct mechanical relaxations in Nafion observed at temperatures T_β and T_α.[24] Eisenberg and co-workers[22] attributed these endothermic events to the glass transition temperature of the matrix (ca. 140 °C) and of the ionic domains (ca. 240 °C). Moore and Martin[7] also observed two endotherms at ca. 150 and 260 °C, which, in agreement with the assignments of Eisenberg, were attributed to the matrix ($T_{g,m}$) and ionic domain ($T_{g,c}$) glass transitions, respectively. In these studies, the position of the high-temperature endotherm was shown to change as a function of processing conditions and counterion type. The drop in $T_{g,c}$ for recast Nafion (i.e., low-temperature solvent evaporation), when compared to solution processed (i.e., high-temperature solvent evaporation) and as-received Nafion, was attributed to a smaller fraction of ionic groups present in the cluster phase.[7] It was assumed that ionic groups not incorporated into the cluster phase exist as small multiplets and/or isolated ion pairs in the matrix such that they do not yield a significant contribution to the apparent cluster transition.[7]

A recent DSC study by de Almeida and Kawano[20] of the thermal behavior of Nafion membranes revealed two endothermic peaks upon first heating, occurring at 120 and 230 °C. The peak at 120 °C did not appear upon reheating but reappeared gradually as the sample was annealed. Because of the dependence of this peak on counterion and hydration level, it was assigned to an order−disorder transition inside the clusters, while the peak at ca. 230 °C was attributed to the melting of the crystallites in Nafion.

Similar studies have been carried out on perfluorosulfonate ionomers, that contain a shorter perfluoroether side chain than Nafion, of varying equivalent weights originally produced by the Dow Chemical Co. For the Dow PFSI's, Moore and Martin[11] observed two, or three, endotherms depending on the equivalent weight of the ionomer. The lowest temperature endotherm (150−180 °C) was assigned to the matrix glass transition temperature ($T_{g,m}$), and the second endotherm (270−300 °C) was attributed to the glass transition temperature of the ionic domains ($T_{g,c}$). The high equivalent weight ionomers showed an endotherm at ∼335 °C, which was determined to be the melting of PTFE-like crystallites.

Mauritz and co-workers[27−30] also used DSC and dielectric spectroscopy to study the Dow perfluorosulfonate ionomers. In particular, they examined the effect of annealing on the DSC and dielectric relaxations of the Dow PFSI's. In agreement with the work of Moore and Martin, the DSC thermograms revealed three endotherms that were attributed to the matrix glass transition temperature, $T_{g,m}$ (215−240 °C), the ionic domain glass transition, $T_{g,c}$ (282 °C), and the melting of crystallites, T_m (332−338 °C). Changes in the DSC thermograms upon annealing at different temperatures were ascribed to microstructural reorganizations in the matrix and/or the cluster phase. They observed an increase in both $T_{g,m}$ and T_m with an increase in the annealing temperature (T_a). It was suggested that during annealing the homogeneity and order in the matrix increases at the expense of the structural order in the side-chain packing. Shifts in peak intensities and relaxation times in the dielectric spectra of these materials were correlated to the changes observed in the endotherms measured by DSC.

The mechanical properties of Nafion and its sulfonyl fluoride precursor (i.e., the melt-processable, nonionic form of the copolymer) have been the source of many investigations.[2,21,24−26,31,32] The Nafion precursor differs from the ionomer in that the perfluoroether side chain is terminated with a nonionic SO_2F group rather than the highly polar SO_3H group. Using dynamic mechanical analysis (DMA), Eisenberg and Hodge[21] found the precursor to display three major relaxations (γ, β, and α) over the temperature range from −196 to 70 °C. The low-temperature relaxation, γ, at approximately −190 °C was attributed to motions of the SO_2F group. The β relaxation was found to be a broad peak in the range from −100 to −20 °C. At low frequencies, this peak could be resolved into two components. Because of the dual-component nature and breadth of this relaxation, it was attributed to local motions of the backbone and side chain. The dominant α relaxation (at ca. 20 °C) was attributed to the glass transition of the polymer.[21]

Eisenberg and co-workers[22,24] also studied the effect of ionization and neutralization on the DMA of Nafion polymers. In early studies,[24] three relaxation peaks ($\alpha > \beta > \gamma$), in the temperature range from −160 to ca. 150 °C, were observed for the acid form of Nafion. Both α and β relaxations were observed to increase by over 100 °C when neutralized with alkali salts, while the low-temperature γ relaxation remained unaffected by neutralization. Because of the strong effect of water on the β relaxation, the peak was attributed to a relaxation of the ionic domains, while the α and γ relaxations were attributed to the glass transition temperature of the fluorocarbon matrix and short-range motions of the $-CF_2-$ backbone, respectively.[24] In a later study involving partially ionized and neutralized Nafion, Eisenberg and co-workers[22] reversed the assignments of the α and β relaxations, while the assignment for the low-temperature γ relaxation remained the same.

Miura and Yoshida[31] conducted a study focused on the effects of solvents (water and alcohol) on the molecular motions in Nafion neutralized with inorganic and organic ions using DMA. In this study, the α relaxation was found to have a strong dependence on counterion type, and absorption of a solvent affected the α, β, and the γ relaxations. In agreement with the work of Eisenberg,[22] the molecular origins of the two high-temperature relaxations, α and β, are attributed to the glass transition of the ionic regions and the matrix, respectively, while the low-temperature relaxation, γ, was attributed to local motions of the PFTE-like backbone.[22]

Because of the technological importance of perfluorosulfonate ionomers (particularly in the field of PEM fuel cells), accurate assignments of the thermal transitions and mechanical relaxations in Nafion to specific molecular/morphological origins is critical to the fundamental understanding of structure−property relationships in these materials. To date, however, the limited reports on this subject have been rather vague and contain significant inconsistencies based on inaccurate correlations between DSC and DMA data. Despite the excellent agreement noted between DSC and DMA, our recent work[33] has shown that the two DSC endothermic transitions disappear upon immediate rescan (in agreement with the observations of de Almeida and Kawano), while the relaxations observed

in DMA persist. This simple observation certainly calls into question the previous assignments of the thermal transitions and mechanical relaxations in Nafion. If the transitions/relaxations observed in both DSC and DMA are probing the same molecular processes, then it would be logical for the transitions in the DSC to remain upon immediate rescan. Because of this inconsistency, it is reasonable to conclude that an alternative explanation for the origins of the endothermic events must exist. Furthermore, given the wealth of morphological and molecular-level information now available with modern instrumentation, more precise assignments of the dynamic mechanical relaxations should be possible.

Over the past 30 years, a wide variety of studies involving perfluorosulfonate ionomers have aimed to link the thermal, mechanical, and other properties (i.e., transport, ionic conductivity, and dielectric behavior) to ramifications of specific morphological features.[20−22,24,25,27−30] Currently, a significant concern regarding the "glass transition temperature" of Nafion has arisen with respect to potential limitations of this polymer in elevated-temperature fuel cell applications. Therefore, it is necessary to define the current understanding of the origins of thermal transitions and mechanical relaxations in perfluorosulfonate ionomers, as this understanding plays a key role in the interpretation of the effect of thermal treatment on the properties of these materials. To address this need, the purpose of this investigation is to reconcile the differences observed in the thermal behavior of Nafion as measured by DSC and DMA and to offer a more precise explanation as to the molecular origins of the endotherms and relaxations in DSC and DMA, respectively, through specific correlations with variable-temperature SAXS and ^{19}F solid-state NMR techniques. Ultimately, this program of research seeks to provide a fundamental understanding of the link between electrostatic interactions and thermomechanical properties in Nafion, thus advancing the current state of understanding of the properties of PFSI materials.

Experimental Section

Materials. Nafion 117 (1100 EW, sulfonic acid form) and its nonionic precursor were obtained from E.I. DuPont de Nemours & Co. The tetramethyl (TMA^+), ethyl (TEA^+), propyl (TPA^+), and butylammonium (TBA^+) counterions were obtained from Aldrich in the form of hydroxides dissolved in either water or methanol. The tetrapentyl ($TPentA^+$), hexyl ($THexA^+$), heptyl ($THepA^+$), octyl ($TOctA^+$), and decylammonium ($TDecA^+$) counterions were obtained from Aldrich as bromide salts. All other reagents were obtained from Aldrich and used without further purification.

PFSI Sample Preparation. The PFSI membranes were cleaned by refluxing in 8 M HNO_3 for ca. 12 h. These H^+-form membranes were then washed with deionized (DI) water to remove excess acid. After drying, the samples were neutralized with aqueous NaOH solution and rinsed with DI H_2O. The Na^+-, K^+-, Rb^+-, and Cs^+-form PFSIs were prepared by soaking the HNO_3-treated membranes in 1 M solutions of the appropriate group 1A hydroxide in methanol. For experiments involving as-received membranes neutralized with TMA^+, TEA^+, TPA^+, etc. counterions, the membranes were prepared by soaking the H^+-form membranes in excess (ca. 5×) methanolic solution of the appropriate alkylammonium hydroxide/bromide. The neutralized membranes were thoroughly rinsed of excess alkylammonium hydroxide/bromide and dried in a vacuum oven at 70 °C overnight.

Thermal Analysis. DSC data were collected on a Perkin-Elmer DSC-7 at 20 °C/min under N_2 purge. Initial DSC thermograms were obtained after thoroughly drying the samples (in the DSC) at 120 °C for 2 h. For annealing experiments, previous sample history was erased by first heating the samples to 330 °C, holding for 5 min, and then cooling back to ambient temperature. The ionomers and sulfonyl fluoride precursor were then annealed at 200 °C for $^1/_2$, 2, 6, 12, and 24 h. To evaluate the effect of annealing temperature on the PFSI crystallization, the annealing times were kept constant (2 h), and the annealing temperature was varied between 120 and 240 °C (at 30 °C intervals).

Dynamic mechanical measurements were performed using a Seiko Instruments SDM 5600 series dynamic mechanical spectrometer (DMS 200). Membrane samples were analyzed in the tensile mode at a frequency of 1 Hz and a heating rate of 5 °C/min.

Small-Angle X-ray Scattering (SAXS). Variable temperature, time-resolved small-angle X-ray scattering was performed at the Brookhaven National Laboratory on the Advanced Polymer Beamline (X27C) at the National Synchrotron Light Source. The incident X-ray beam was tuned to a wavelength of 0.1366 nm, and the sample-to-detector distance was 85 cm. The two-dimensional scattering images were recorded using a Mar CCD camera with an intensity uncertainty on the order of 2%. The Nafion samples were heated in a sample chamber in the X-ray beam at a heating rate of 5 °C/min with an uncertainty of ±1 °C while acquisition times were kept to 1 min, and data were recorded from 50 to 300 °C. Intensity vs pixel data were obtained from the integration of the 2-D images using the POLAR software developed by Stonybrook Technology and Applied Research, Inc. The relationship between pixel and the momentum transfer vector q was determined by calibrating the scattering data with a silver behenate standard. All scattering intensities were corrected for transmission, incident beam flux, and background scatter due to air and Kapton windows. SAXS studies on Na^+-form Nafion, in connection with the annealing studies, were also collected at the Stanford Synchrotron Radiation Laboratory. The scattering profiles were corrected for transmission and background scatter and are represented in arbitrary, relative intensity units as a function of the scattering vector, q, which is a function of the scattering angle through the following relationship

$$q = \frac{4\pi}{\lambda}\sin(\theta) \tag{1}$$

where λ is the wavelength of radiation (0.1366 nm) and θ is half of the scattering angle (2θ). Because of an increase in the scattering intensity at large q arising from thermal density fluctuations, Porod analysis was performed on each scattering curve in order to account for this baseline intensity, I_b. Porod's law states that at large q the scattering intensity is proportional to q^{-4} for a two-phase system with sharp phase boundaries.

$$\lim_{q\to\infty} I(q) \propto q^{-4} \tag{2}$$

More specifically, the following equation was used to determine the intensity arising from thermal density fluctuations (I_b)

$$\lim_{q\to\infty} I(q) = \frac{K}{q^4} + I_b \tag{3}$$

where q is the scattering vector, K is Porod's constant, which is related to the interphase of the scattering entities, and I_b is the background scattering intensity. From a plot of $I(q)q^4$ vs q,[4] a linear regression was performed and the slope of the line was taken as I_b, which was then subtracted from the scattered intensity.

Solid-State ^{19}F NMR Spectroscopy. Solid-state ^{19}F NMR was performed on a Varian Unity-Inova 400 MHz spectrometer using the ^1H channel of a Chemagnetics H-X-Y 4 mm triple-resonance probe. The probe circuit was tuned to 376 MHz for ^{19}F detection. Samples were loaded into zirconia cylinder rotors sealed with Torlon drive tips and Teflon caps and spun at 10.5

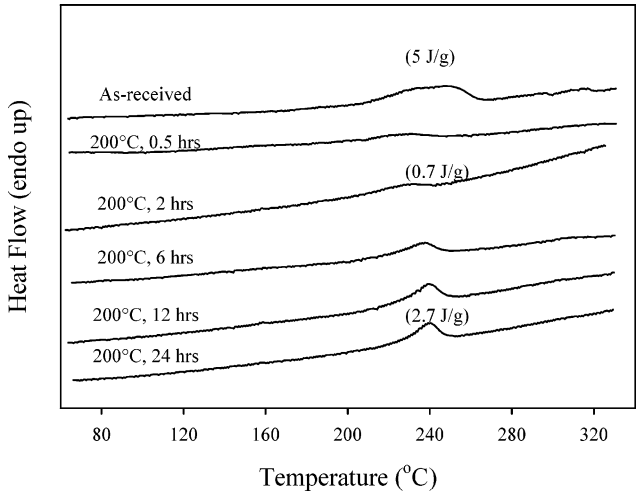

Figure 1. DSC thermograms of Na^+ form Nafion 1100 annealed at 200 °C for various times. Thermograms are shifted along the *y*-axis for comparison.

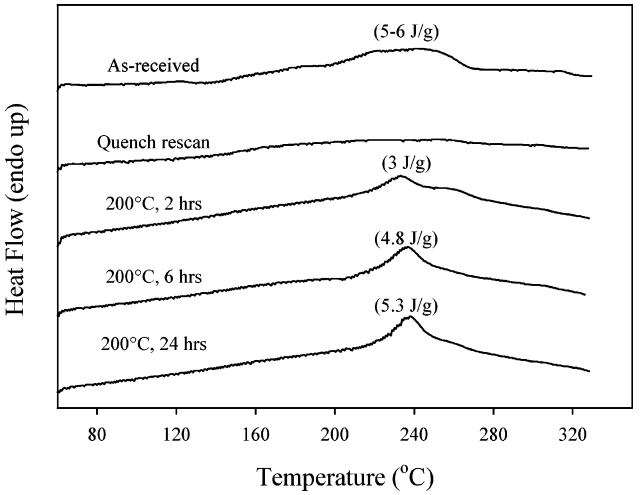

Figure 2. DSC thermograms of Cs^+ form Nafion 1100 annealed at 200 °C for various times. Thermograms are shifted along the *y*-axis for comparison.

kHz. Spin-diffusion data were acquired using the DANTE sequence[34] to selectively invert the resonance associated with ^{19}F nuclei in the side chain as well as its sidebands. In both the sideband and spin-diffusion experiments the DEPTH pulse sequence[35] was used to remove ^{19}F background contributions from the cap and probe body. The acquisition parameters were as follows: the ^{19}F 90° pulse width was 3.1 μs, the acquisition time was 32 ms, the recycle delay ranged from 5 to 6 s, and the number of scans acquired for each data set was 32. The spectral width was set to 500 kHz, and peak positions were referenced externally to C_6F_6. In the ^{19}F NMR spectrum, the peaks at approximately −77 and −120 ppm are attributed to the $-OCF_2$ and $-CF_3$ nuclei in the side chain and the $-CF_2$'s in the backbone, respectively.

For the spin-diffusion studies, the peak at −77 ppm was inverted, and spin magnetization was allowed to transfer to the backbone fluorines. The intensity of the resonance at −77 ppm was monitored as a function of the delay time and normalized by the following equation

$$\Delta M_s(t_{sd}) = \frac{M_x(t_{sd}) - M_{eq}}{M_x(t_{sd} = 0) - M_{eq}} \quad (4)$$

where $M_x(t_{sd})$ is the measured intensity at some delay time, $M_x(t_{sd} = 0)$ is the maximum inverted intensity, and M_{eq} is the intensity of the inverted peak after spin equilibrium has been achieved. Spin-diffusion times (t_{sd}) were calculated by fitting a line to the initial linear region of a plot of the normalized intensity vs the square root of time.[36,37]

Results and Discussion

Differential Scanning Calorimetry. Figures 1 and 2 show the results obtained from DSC for Na^+ and Cs^+ neutralized forms of Nafion 1100 EW in both the as-received state and after thermal treatment. In both cases the initial scan of the as-received materials displays a broad endotherm between 200 and 250 °C. This endotherm disappears upon rescan but can be induced to reappear by annealing at 200 °C (after melt-quenching from 330 °C) for extended periods of time. In agreement with the thermal behavior of semicrystalline polymers with slow crystallization kinetics, this endotherm is assigned to the melting of PTFE-like crystallites and is discussed in detail for each sample.

For Na^+-form Nafion the samples were melt quenched from 330 °C to an isothermal annealing temperature of 200 °C for 0.5, 2, 6, 12, and 24 h. The DSC thermograms (Figure 1) reveal that the heat of fusion (ΔH) for the initial endothermic event is ca. 5 J/g in the as-received material and is virtually nonexistent for the sample which was quenched to 200 °C and annealed for 30 min. Upon annealing at 200 °C for 2 h the ΔH increases to a value of 0.7 J/g and plateaus at a value of 2.7 J/g after 24 h of annealing. These data show that the crystallinity developed during annealing only reaches about 50% of its initial value. The assignment of this endothermic event to the developing crystallinity is confirmed by the small-angle X-ray scattering data obtained for the annealed Na^+-form Nafion samples. Figure 3 shows the relative scattering intensity as a function of the scattering vector, q. The broad shoulder observed for as-received Nafion at a q range of 0.3−0.7 nm^{-1} has been attributed to scattering from crystalline lamellae (i.e., the crystalline long spacing) present in the sample.[5,8] Upon quenching from 330 °C, this shoulder completely disappears and begins to reappear, however not to the same extent, after 24 h of annealing at 200 °C. This behavior is in close agreement with that observed in the DSC results of Figure 1. Thus, the agreement of these complementary techniques strongly supports the assignment of the melting endotherm observed in the DSC to the existence of crystallinity in the sample.

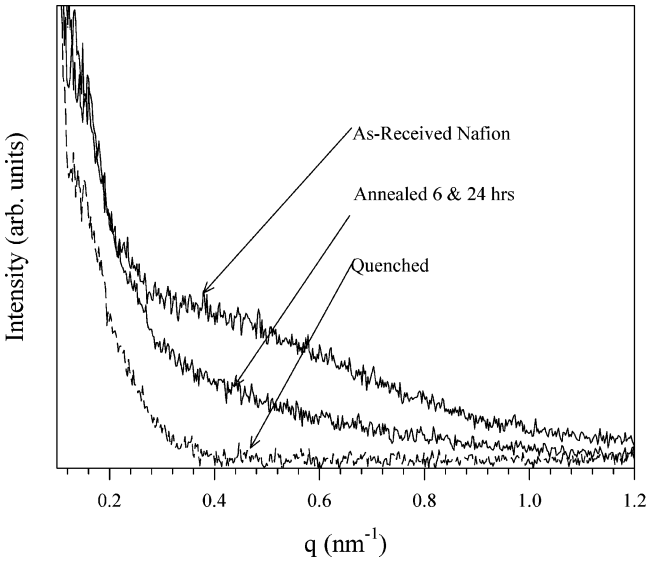

Figure 3. Effect of thermal treatment on the SAXS profiles of Na^+ form Nafion 1100.

Results obtained for annealing studies of Cs^+-form Nafion are presented in Figure 2. Samples were annealed at 200 °C for 2, 6, and 24 h after quenching from 330 °C. As in the case for Na^+-form Nafion, the initial ΔH value for the broad endothermic event (200−250 °C) for the as-received membrane is ca. 5−6 J/g, which can be seen in the DSC thermograms in Figure 2. Upon a quench rescan, the endotherm is no longer present; however, the peak begins to reappear after annealing for longer periods of time. The maximum value ΔH value is reached after 24 h (5.3 J/g) of annealing and is quite comparable to the initial value (5−6 J/g). This shows that, in the case of the Cs^+ counterion, the degree of crystallinity approaches that of the as-received state.

The annealing studies of melt-quenched Na^+- and Cs^+-form Nafion show only a single endothermic event, unlike the DSC data presented in earlier studies, which often show two endothermic events, depending on thermal history. This endothermic event is attributed to melting of PTFE-like crystallites in the presence of an electrostatic network. The influence of the strength of this network is revealed by the fact that the Na^+-form samples do not recover the entire amount of crystallinity when compared to the as-received materials, whereas the Cs^+-form recovers most of its crystallinity after annealing for long periods of time. This behavior is in excellent agreement with our model semicrystalline ionomers studies on sulfonated syndiotactic polystyrene (SsPS).[38,39] In these studies, the randomly incorporated sulfonate groups along the backbone were shown to act as noncrystallizable, interactive defects, which are capable of forming thermally labile, electrostatic cross-links. Changing the counterion associated with the sulfonate groups can vary the strength of these cross-links (by affecting the dipole−dipole interactions) and thus was shown to drastically change the kinetics of crystallization. For example, the Cs^+-form SsPS was shown to crystallize faster than the Na^+-form SsPS due to the greater mobility in the Cs^+ ionomer. It is apparent from the data in Figures 1−3 that Nafion behaves like a model ionomer with regards to the development of crystallinity. Weaker electrostatic interactions facilitate chain mobility that in turn increases the rate of crystallization.

To explain the origins of the multiple endothermic events often observed in the DSC analysis of Nafion, variable temperature annealing studies were conducted with Cs^+-form Nafion. Figure 4 shows the DSC results obtained for as-received samples that were scanned from 50 to 330 °C directly after annealing at temperatures ranging from 120 to 240 °C for 2 h. The data show that, under these specific thermal treatments (i.e., typical of standard drying conditions prior to analysis), two endothermic events can be observed in Nafion. For each treatment, the low-temperature endotherm is observed to occur at ca. 20−30 °C above the respective annealing temperature, while the high-temperature endotherm remains reasonably constant at ca. 240−250 °C. At low annealing temperatures (i.e., 120 °C), the low-temperature endotherm resembles a step change (reminiscent of a T_g with apparent enthalpic relaxation). Given this characteristic profile, it is not surprising that this endothermic event has been attributed to a T_g event for samples dried near 120 °C. However, with higher annealing temperatures, the endothermic event increases in temperature and develops into a distinct peak, characteristic of a melting transition. It is important to note that multiple melting behavior is not uncommon and has been observed in a variety of semicrystalline polymers.[40−45] Thus, we attribute the low-temperature endotherm to melting of small imperfect crystals, similar to that observed in other crystallizable copolymers. At a given annealing temperature (i.e., the isothermal crystallization temperature), a certain population of relatively thin lamellae is formed in "thermal equilibrium" with the annealing temperature. By increasing the annealing temperature, the thin lamellae become thicker resulting in an increase in their T_m. Thus, in contrast to previous assignments, these data support the conclusion that the lower temperature endotherm is due to the melting of small crystallites that develop in the sample due to the annealing conditions, rather than to the matrix T_g of Nafion, as earlier suggested.

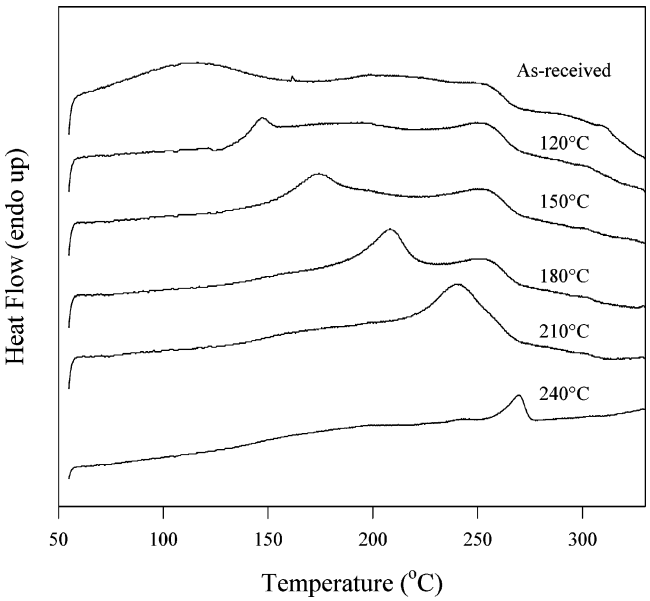

Figure 4. Effect of annealing temperature on DSC thermograms of Cs^+ form Nafion 1100 annealed for 2 h. Thermograms are shifted along the *y*-axis for comparison.

Dynamic Mechanical Analysis (DMA). As previously stated, the physical properties of the sulfonyl fluoride precursor can be significantly altered upon conversion of the $-SO_2F$ groups to the $-SO_3H$ form, and subsequent neutralization can lead to further changes in the physical properties. For example, a wide range of relaxation temperatures can be observed in the tan δ vs temperature plot in Figure 5. These data show an increase of 100 °C for the α transition when the precursor is converted to the acid form and a further increase of ca. 140 °C when the acid form membrane is neutralized with Na^+. The Na^+-form Nafion shows a distinct α (ca. 240 °C) and weak β (ca. 150 °C) relaxation. Previous work has shown that neutralization of Nafion 1100 EW with a range of alkali metal ions (Na^+, K^+, Rb^+, Cs^+) shows little change in the α and β relaxation temperatures.[33]

To explore the influence of the strength of electrostatic interactions on the dynamic mechanical behavior and to elucidate the molecular origins of these relaxations, Nafion membranes were neutralized with a series of protonated alkylammonium counterions. The results obtained from DMA of these samples can be seen in Figure 6A,B. Figure 6A shows plots of the storage modulus vs temperature for TMA^+, TEA^+, TPA^+, TPen-

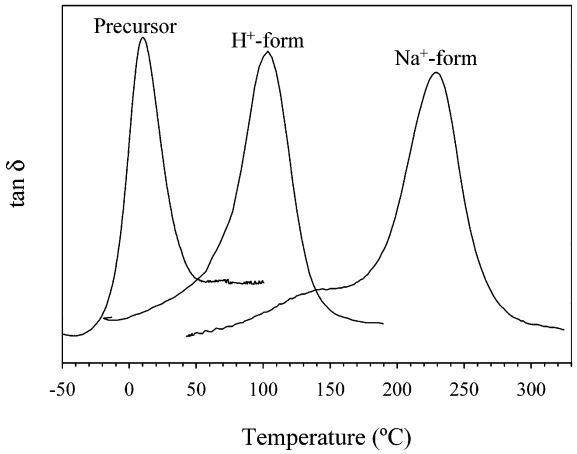

Figure 5. Influence of hydrolysis, neutralization, and electrostatic interactions on the mechanical properties of Nafion.

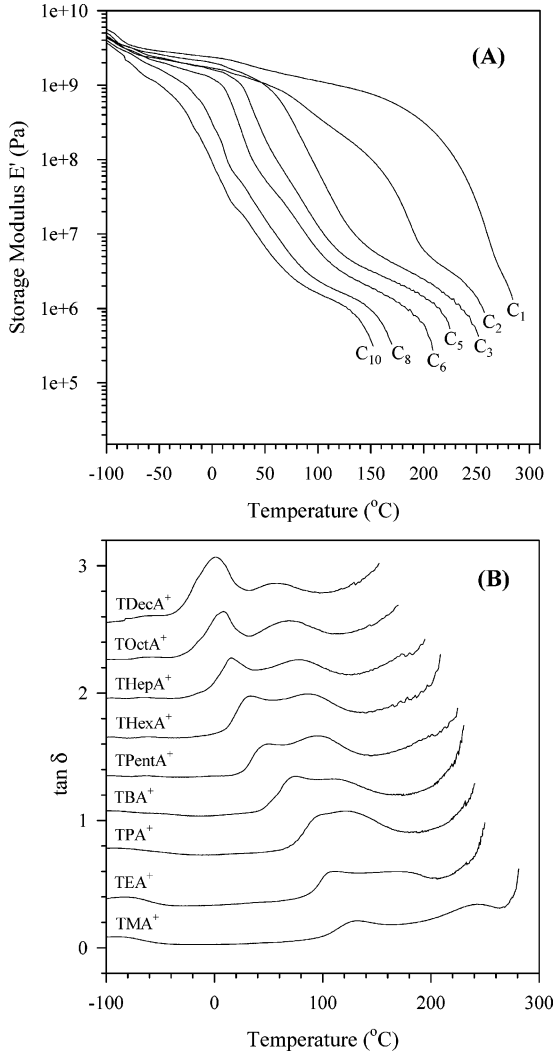

Figure 6. Effect of alkyl chain length on the dynamic mechanical behavior of Nafion neutralized with alkylammonium ions in plots of the (A) storage modulus vs temperature and (B) tan δ vs temperature. Traces are shifted along the *y*-axis for comparison.

tA$^+$, THexA$^+$, TOctA$^+$, and TDecA$^+$ neutralized Nafion. As the size of the counterion increases, the temperature at which the storage modulus drops by several orders of magnitude decreases across the entire temperature range measured. The effect of counterion size is most significant in the rubbery modulus and the terminal region. It is important to note that TGA studies run under similar conditions have shown that these organic counterions are stable in Nafion at temperatures in excess of 300 °C, and thus thermal degradation is not a contributing factor in these rheological or morphological (see below) studies.[33,46]

With these organic counterions, there are two contributing factors by which the physical properties can be affected. As the size of the counterion increases, (1) the larger counterions significantly decrease the strength of the electrostatic interactions (i.e., weaken the electrostatic network) and (2) the bulky, organic counterions can effectively plasticize the material, thus decreasing the relaxation temperatures. For alkylammonium ions of intermediate size (e.g., TBA$^+$), it is likely that both factors contribute to the overall rheological behavior. In an analogous study, Weiss et al.[47] observed an increase in the melt index of alkylamine neutralized polystyrene ionomers with an increase in the bulkiness of the counterion and found that for smaller counterions electrostatic interactions predominate, while the plasticization phenomenon is more important as the counterion becomes sufficiently bulky.

Figure 6B shows the tan δ vs temperature plots for Nafion neutralized with TMA$^+$, TEA$^+$, TPA$^+$, TBA$^+$, TPentA$^+$, THexA$^+$, THepA$^+$, TOctA$^+$, and TDecA$^+$. In contrast to the data observed for the Na$^+$-form Nafion (Figure 5), all of the organic ions yield two distinct peaks with well-resolved β and α relaxations. For the smallest TMA$^+$ counterion, the α relaxation occurs at a temperature quite comparable to that observed for the Na$^+$-form sample; however, the β relaxation is much more pronounced and occurs at a temperature 50 °C lower than that of the Na$^+$-form sample. As the size of the alkylammonium ions increases, the peak maximum (for each relaxation) shifts to lower temperatures, in a fairly parallel fashion. In contrast to the typical preferential plasticization effect of ionic or polar additives in other ionomer systems (i.e., a reduction in the α relaxation temperature with little effect on the β relaxation), the behavior of Nafion containing the alkylammonium counterions indicates that molecular origins of *both* the α and β relaxations are coupled to the influence of the ionic groups.

In addition to the decrease in relaxation temperatures with increasing counterion size, there is also a profound increase in the relative intensity of the β relaxation as the size of the counterion increases. While the α relaxation is dominant in the Na$^+$-form sample, the β relaxation becomes dominant for the systems containing the largest organic ions. This inversion in dominance suggests that as the counterion size increases, larger populations of chains are capable of activated motion at lower temperatures. Within the context of a nanophase-separated morphology, this behavior may be attributed to very weak associations between ion pairs for the systems containing the large counterions (i.e., a weak electrostatic network). With weakened interactions between the ionic groups, the efficiency of the physical cross-links to locally restrict the mobility of chains decreases, yielding a relatively larger population of chains in a more mobile state. An extreme extension of this trend is evident in the DMA behavior of the nonionic precursor (Figure 5); without electrostatic cross-links, only one low-temperature relaxation is observed (near 0 °C).

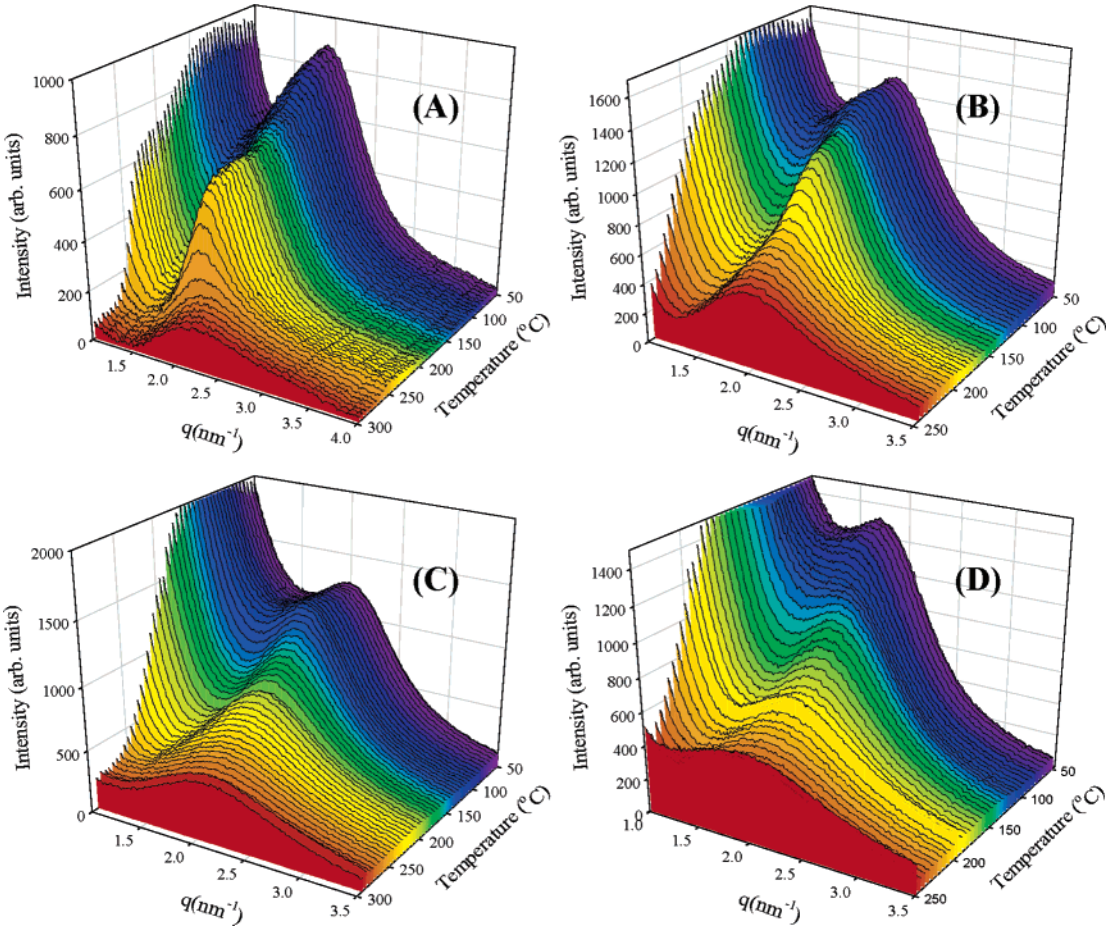

Figure 7. Variable temperature SAXS for (A) TMA^+, (B) TEA^+, (C) TPA^+, and (D) TBA^+.

Table 1. Transition Temperatures Measured by DMA, ^{19}F NMR, and SAXS for TMA^+, TEA^+, TPA^+, and TBA^+ Nafion

	DMA		^{19}F NMR		
	α	β	side chain	main chain	SAXS
TMA^+	240	130		150	240−260
TEA^+	160	111	200−225	140	165−185
TPA^+	130	100	150−175	110	120−130
TBA^+	100	73	125−150	100	80−100

Small-Angle X-ray Scattering (SAXS). To develop a fundamental understanding of the link between electrostatic interactions and the thermomechanical properties of Nafion, and ultimately the molecular origins of the mechanical relaxations, it is important to understand how the ionomer morphology behaves as a function of temperature. Therefore, variable temperature SAXS experiments were carried out for TMA^+, TEA^+, TPA^+, and TBA^+ Nafion, the results of which can be seen in Figure 7A−D. Scattering profiles were obtained over a temperature range of 50−300 °C (i.e., the same temperature range for the DMA experiments). The peak at $q \approx 2$ nm^{-1} is the ionomer peak attributed to a scattering maximum from the interparticle interference characteristic of the existence of ionic aggregates that are spatially distributed throughout the sample.

Figure 7 shows that the temperature dependence of the ionomer peak is greatly influenced by the counterion size. For each neutralized form of Nafion, there is an abrupt decrease in the scattering intensity with increasing temperature, and the temperature range over which this sudden change occurs (see Table 1) decreases with increasing counterion size. From these data, it is apparent that the temperature dependence of the ionomer morphology depends highly on the counterion used in the neutralization. At elevated temperatures, the elastic forces exerted upon the chains emanating from the ionic aggregates tend to increase to a point that exceeds the electrostatic attractive forces between ion pairs in the aggregate. As a result of this destabilizing condition, the *static* electrostatic network (i.e., a network of physically cross-linked chains with ion pair junction sites securely connected to stable ionic aggregates) transitions to a *dynamic* network through the process known as ion-hopping (i.e., the thermally activated process of ion pairs "hopping" from one aggregate to another in order to relieve local stress).[48,49] With increasing thermal energy, the mobility of ion pairs increases such that, under the time scale of the SAXS experiment (1 min per scan), the time-averaged distribution of ion pairs becomes more homogeneous and thus the ionomer peak decreases in intensity. With increasing counterion size, and thus weakened interactions, the temperature at which this activated process occurs decreases. As seen in the data of Table 1, the observed temperatures of these morphological transitions correlate strongly with the temperatures of the α relaxations for the series of alkylammonium ion forms of the ionomer.

^{19}F Solid-State Nuclear Magnetic Resonance (SSNMR). To establish molecular origins for the thermomechanical properties of Nafion and to understand the link between electrostatic interactions and molecular motions (which ultimately influence the physical properties), it is necessary to use a molecular-level probe

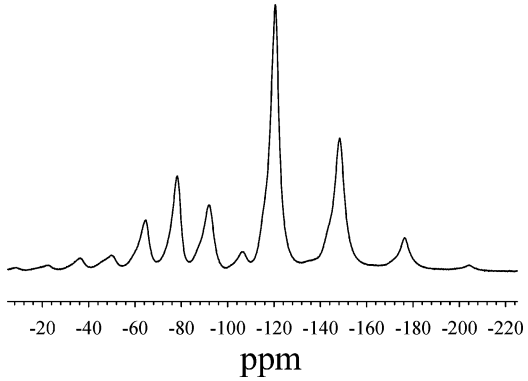

Figure 8. ^{19}F SSNMR spectrum for Nafion (1100 EW) spun at 10.5 kHz using a 400 MHz spectrometer.

as provided by ^{19}F SSNMR spectroscopy. To date, NMR has been used to investigate several aspects of Nafion, which have included structure and dynamics,[37,50−53] morphology and transport,[36,54−59] and aspects of the counterion associated with the sulfonate group.[60−63] In this study, variable temperature solid-state ^{19}F NMR is used to evaluate the motions of the perfluoroether side chains using spin-diffusion and sideband analysis over the same temperature ranges as used in the DMA and SAXS analyses. The ^{19}F spectrum for Nafion can be seen in Figure 8, and the peaks at approximately −77 ppm and −120 ppm are attributed to the $-OCF_2$ and $-CF_3$ nuclei in the side chain and the $-CF_2$'s in the backbone, respectively.[50]

Spin-diffusion studies have typically been used to determine domain sizes in two-phase systems.[64] Recently, Inglefield and co-workers[36] have attributed an increase in the spin-diffusion times (t_{sd}) in hydrated Nafion to an increase in the size of the ionic domains with various levels of hydration. The two main assumptions in this study were that (i) the two phases consist of a polar region containing the perfluoroether side chain and a region containing the PTFE-like backbone and (ii) the ionomer morphology of Nafion is lamellar. In the present variable temperature study of dry samples, we recognize that the distance between coupled side-chain and main-chain fluorine nuclei is essentially constant (due to the specific chemical structure of 1100 EW Nafion). Thus, we attribute changes in spin-diffusion times to changes in the mobility of the polymer chains. With increasing chain mobility, the spin−spin interactions between the ^{19}F nuclei in the side chain and those of the main chain decrease due to reduced dipolar coupling.

Figure 9 shows spin-diffusion time as a function of temperature for Na^+, TMA^+, and TBA^+ neutralized Nafion samples. These data indicate that the temperature dependence of the spin-diffusion time is greatly influenced by the size of the counterion associated with the sulfonate group. Below about 100 °C, each of the counterion forms yield the same spin-diffusion times. However, above a particular temperature (referred to here as T_c), a nonlinear increase in t_{sd} is observed for both the TMA^+ ($T_c \approx 180$ °C) and TBA^+ ($T_c \approx 100$ °C) form Nafion. In contrast, the Na^+-form Nafion maintains a relatively constant spin-diffusion time. In agreement with the DMA and SAXS results, the increase in t_{sd}, at the temperature T_c, for the TMA^+ and TBA^+ forms of Nafion may be attributed to an onset of molecular motions. This increase in mobility effectively decreases the spin−spin coupling between the side- and main-chain fluorines leading to increased t_{sd}'s. For the Na^+-form Nafion, the mobility within the static electrostatic network remains relatively low; therefore, there is little change in the spin-diffusion times. The sidebands associated with the ^{19}F resonances may also be used to probe the molecular motions of the polymer chains in Nafion. Sidebands arise due to dipolar coupling, and the intensity of these peaks is a function of the rigidity in solids. Typically, magic-angle spinning (MAS) experiments are carried out in order to average out the contribution of these dipolar interactions to the spectrum. If the spinning rate of the sample is larger than the dipolar interactions, then the sidebands are separated from the isotropic resonance peak and becoming smaller in intensity with increasing spinning rate.[65] However, the mobility of the polymer chains can also affect the intensity of the sidebands. As the material becomes more mobile, the dipolar interactions become more isotropic, and therefore the sidebands begin to disappear. This phenomenon is used here to observe changes in mobility in Nafion.

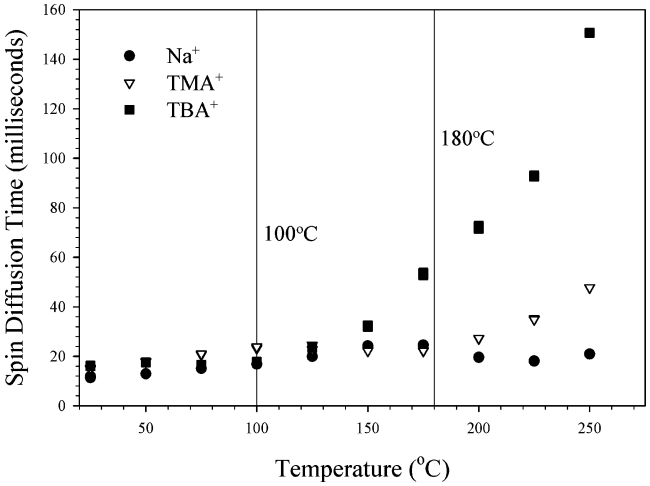

Figure 9. Temperature dependence of the spin-diffusion time (t_{sd}) for (●) Na^+, (▽) TMA^+, and (■) TBA^+ Nafion.

An example of the effect of temperature on sideband intensity can be seen in Figure 10, which compares the variable-temperature spectra for TMA^+- and TBA^+-form Nafion. The spectra were taken from 25 to 250 °C at 25 °C increments, and the sidebands for the side- and main-chain peaks are denoted by * and **, respectively. These data show that the intensity of the sidebands decrease as the temperature increases. It is also apparent that the sidebands for the TBA^+-form Nafion decrease in intensity much more rapidly than do those for TMA^+-form Nafion. This behavior is attributed to the higher mobility in the TBA^+ Nafion. The higher mobility allows the dipolar coupling to be averaged out more effectively, thus leading to a much more rapid decrease in sideband intensity as a function of temperature.

To quantify the NMR behavior as a function of temperature, the sideband intensities were normalized by the intensity of their respective side and main-chain isotropic resonances, as shown in Figures 11 and 12. For all forms of Nafion the normalized intensities for both the side- and main-chain fluorines show a decrease as the temperature increases. It is also apparent from the graphs that the counterion size has a significant impact on the rate at which the sidebands decrease in intensity.

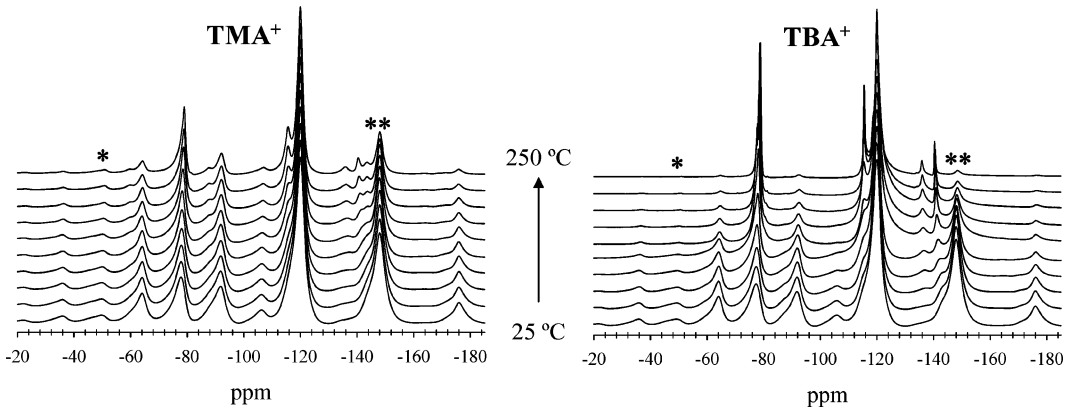

Figure 10. Variable temperature ^{19}F spectra for TMA^+ and TBA^+, taken from 25 to 250 °C every 25 °C, where the sidebands for the side- and main-chain resonances have been denoted by * and **, respectively.

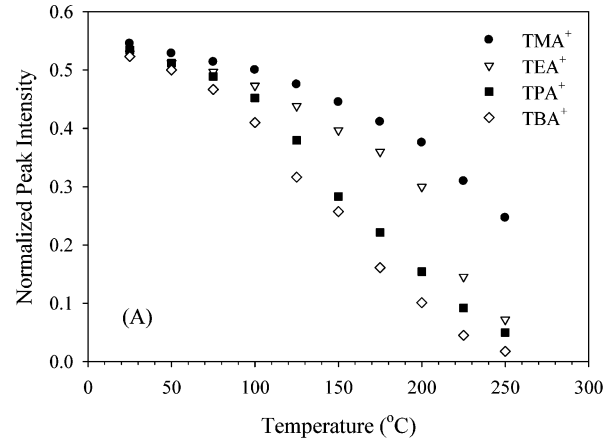

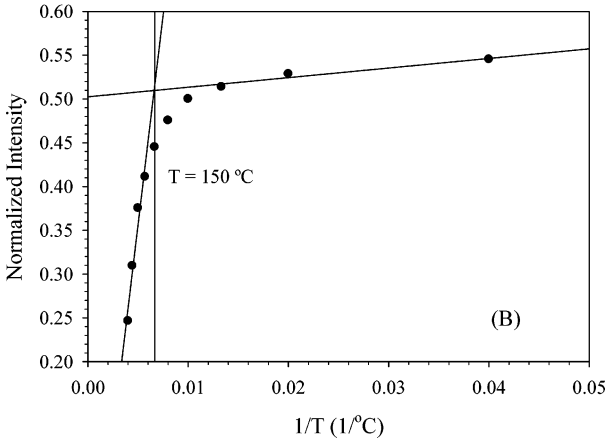

Figure 11. (A) Normalized sideband intensity for the main-chain resonances for (●) TMA^+, (▽) TEA^+, (■) TPA^+, and (◇) TBA^+ Nafion. (B) Determination of the transition temperature for main-chain sidebands by plotting the normalized intensity vs $1/T$, followed by extrapolation.

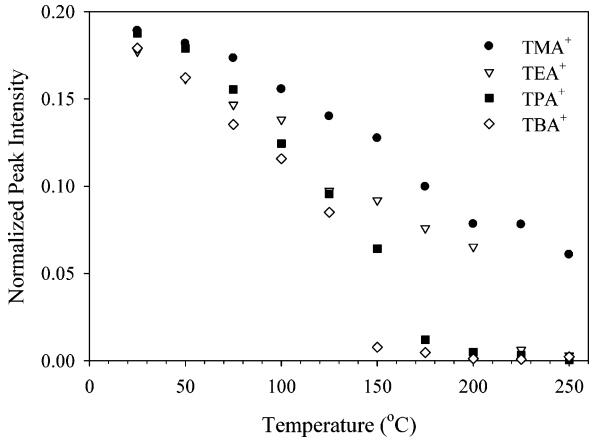

Figure 12. Normalized sideband intensity for the side-chain resonances for (●) TMA^+, (▽) TEA^+, (■) TPA^+, and (◇) TBA^+ Nafion.

For the main-chain sidebands (Figure 11A), the decrease in sideband intensity as a function of temperature is shown to be highly dependent on counterion size. As the size of the counterion increases, the sidebands decrease at a faster rate. At low temperatures the rate of change in the normalized peak intensity is relatively low, while at high temperatures, the rate of change in the normalized peak intensity increases significantly. This change in the rate at which the sidebands decrease may be attributed to a change in dynamics of the backbone. The transition in dynamics was determined by plotting the normalized intensity vs $1/T$ and taking the intersection of the extrapolation from the two linear regions, which can be seen in Figure 11B for TMA^+ Nafion. The transition temperatures for the main chain are listed in Table 1. As the size of the counterion increases, the subsequent increase in chain mobility yields a decrease in the transition temperature (i.e., the temperature at which an apparent onset of significant chain dynamics effectively reduce dipolar coupling). Moreover, it is important to note that these transitions in main-chain dynamics occur at temperatures above the β relaxation temperatures observed in DMA (Table 1).

In comparison to the main-chain behavior, the side-chain sidebands show a markedly different response to temperature. As shown in Figure 12, the intensity of the side-chain sidebands decreases linearly as a function of temperature. Again, the rate of intensity decrease becomes greater as the size of the counterion increases, indicating that side-chain mobility increases with counterion size. At temperatures below ca. 100 °C, the side-chain sidebands are observed to decrease more rapidly than the main-chain sidebands (in comparison with the data in Figure 11A). This indicates that the side chains are inherently more mobile than the main chains, which is supported by recent NMR studies by Schmidt-Rohr and co-workers.[50] At elevated temperatures, the data also show an abrupt drop in intensity for the TEA^+-, TPA^+-, and TBA^+-form samples. With increasing counterion size, the temperature range of the abrupt change in intensity decreases (see Table 1). These drops in intensity suggest a sudden onset of increased mobility of the side chains at these elevated temperatures and

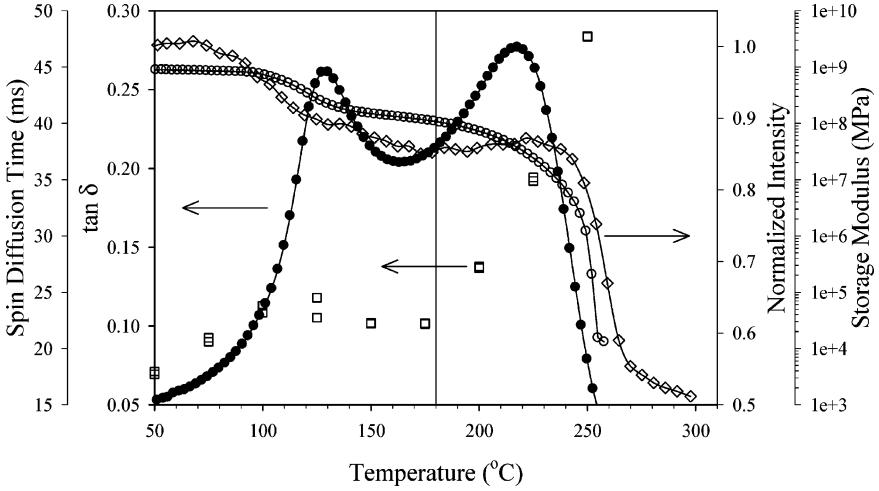

Figure 13. Correlations between (●) DMA (tan δ), (○) DMA (storage modulus), (◇) SAXS, and (□) spin-diffusion times for TMA^+-form Nafion.

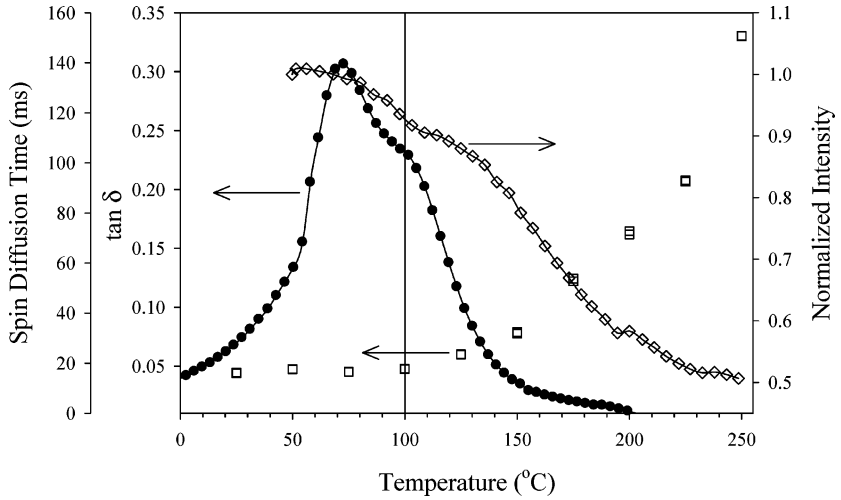

Figure 14. Correlations between (●) DMA, (◇) SAXS, and (□) spin-diffusion times for TBA^+-form Nafion.

may be correlated with the DMA behavior. The data in Table 1 indicate that the onset of significant side-chain mobility occurs at temperatures above the α-relaxations. For the TMA^+-form sample, with the highest α-relaxation, the onset of mobility is likely to occur above the maximum temperature range of the instrument.

While the temperature ranges observed for the side-chain and main-chain transitions (as measured by NMR) are somewhat higher than the α and β relaxations (as measured by DMA), it is important to note that the experimental time scale of dynamics probed by these two methods are significantly different. Since these NMR experiments are probing dynamics on the 10 s of kilohertz time scale and the DMA experiments are probing dynamics on the 1 Hz time scale, the transition temperatures measured by NMR (for a given molecular process) will be observed at significantly higher temperatures relative to DMA measurements.[66] Given this contrast in time scales, it is reasonable to correlate the onset of motions of the side chains and main chains to the α and β relaxations.

Correlations between DMA, SAXS, and ^{19}F SS-NMR. Simply analyzing the DMA as a function of the counterion type and/or solvent content is not sufficient to offer an explanation as to the molecular origins of the mechanical relaxations in Nafion. Therefore, it is necessary to discuss the DMA results along with results obtained from SAXS and NMR. The ionomer peak, observed in SAXS, allows the monitoring of the ionomer morphology as a function of temperature and provides insight into the relationship between the strength of the electrostatic network—dictated by counterion size—and the relaxations observed in DMA. Variable temperature ^{19}F solid-state NMR experiments allow the relaxations and morphological changes to be linked to molecular motions.

Specific correlations between the variable temperature X-ray scattering behavior, ^{19}F NMR spin-diffusion time, and the tan δ for TMA^+- and TBA^+-form Nafion are shown in Figures 13 and 14, respectively. Each figure shows an overlay of the normalized scattering intensity of the ionomer peak, the spin-diffusion time, and the tan δ all as a function of temperature. From these data, it is apparent that the α relaxation in the DMA correlates very well with the drop in intensity of the ionomer peak and that the temperature at which this occurs is strongly dependent on the strength of the electrostatic network, which is established by the size of the counterion. The correlation between the SAXS and DMA data show that the α relaxation in the DMA is due to motions associated with the electrostatic network. Because the ionomer peak persists at temperatures above the β-relaxation, yet virtually disappears above the α-relaxation, it is proposed that the electro-

static network becomes dynamic near the α-relaxation, facilitated by an ion-hopping process as discussed in the literature for ionomers.[48,49] Also, a significant increase in the spin-diffusion time corresponding with the onset of the α relaxation can be seen in both plots. The spin-diffusion studies reveal the onset of molecular motions of the side and main chain, which greatly reduce the amount of spin−spin coupling. From the sideband studies, a sudden drop in the side-chain sideband intensity suggests the onset of significant molecular motions that greatly affect the dipolar interactions; this behavior also coincides with the α relaxation observed in DMA. Thus, the α-relaxation in Nafion may be assigned to the onset of thermally activated motions of the side and main chains facilitated by a profound weakening of the electrostatic attractive forces within the ionic aggregates. For Nafion containing large alkylammonium counterions (with significantly weakened interactions), the chain motions associated with the α relaxation may ultimately lead to a destabilization of the ionic domains (i.e., a transition from a static, physically cross-linked system to a dynamic network). At temperatures above the α relaxation, the side chains experience increased mobility through the process of ion-hopping, and consequently, the ion pairs become more homogeneously distributed. This phenomenon undoubtedly offers the ability to melt-process Nafion containing large alkylammonium counterions.[23]

The data in Figure 6B reveal that the counterion size has a significant effect on not only the α relaxation but also the β relaxation. Although there is little change in the position of the α relaxation in TMA^+ Nafion (ca. 236−246 °C) when compared to Na^+-form (ca. 240−250 °C), the β relaxation shows a significant drop in temperature (ca. Δ50 °C). For the series of organic ions, the β relaxation systematically decreases in temperature and increases in relative intensity with increasing counterion size. This behavior indicates that the β relaxation is significantly influenced by the strength of the electrostatic interactions and thus motions within the ionic domains. Behavior such as this, and others present in the literature, are what has led to some confusion about the molecular origins of these relaxations. When considering the behavior of conventional ionomer systems, the incorporation of ionic plasticizers often show a preferential plasticization of the regions of restricted mobility near the ionic aggregates (i.e., a decrease in the temperature of the α relaxation with little effect on the β relaxation).[67] In the context of the studies discussed here, the organic counterion should behave like a polar ionic plasticizer. If the β relaxation were simply due to the T_g of the matrix (i.e., chains far removed from the ionic domains), as suggested by Eisenberg et al.,[22] then there should be little effect on the β relaxation by changing the counterion. However, the fact that the β relaxation is affected by the counterion size and transitions in backbone dynamics (NMR) have been observed at temperatures correlated to the β relaxation lead to the conclusion that the main-chain motions are strongly coupled, through the side chains, to the restricting effects of the electrostatic cross-links. Furthermore, since there is strong evidence of ionic aggregation at temperatures in the vicinity of the β relaxation (SAXS) and no abrupt changes in side chain mobility (NMR), it can be concluded that these motions occur in the presence of a static network of physically cross-linked chains. Thus, the β relaxation in Nafion

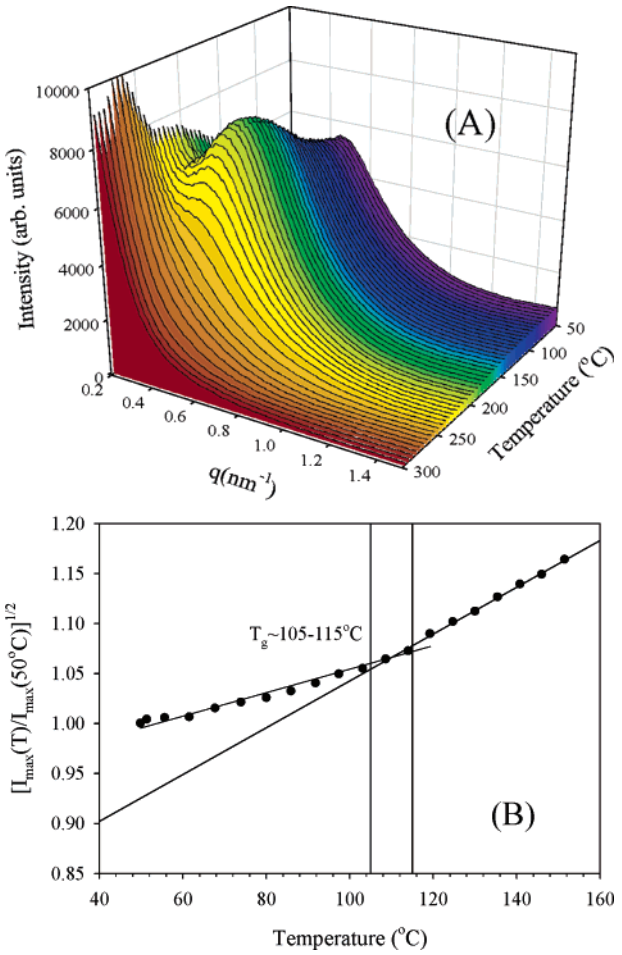

Figure 15. (A) Temperature dependence of crystalline long period peak (0.5 nm^{-1}) for TMA^+-form Nafion and (B) plot of $\sqrt{I_{max}(T)/I_{max}(T_0)}$ vs temperature used to determine the T_g of TMA^+-form Nafion (105−115 °C).

may be assigned to the onset of thermally activated main-chain motions that are facilitated through side-chain mobility within the framework of a static physical (electrostatic) network.

Figure 13 also shows a comparison of the temperature dependence of the normalized intensity of the ionomer peak and the storage modulus for TMA^+-form Nafion. It is important to note that the initial drop in the storage modulus to the rubbery plateau (onset of the β relaxation) coincides with a drop in the intensity of the ionomer peak. Over the same temperature range, the data in Figure 15A show a significant change (increase) in intensity of the low-q peak attributed to intercrystalline domain scattering (often referred to as the long period)[5,8] at ca. 0.5 nm^{-1} as a function of temperature. Although there is a drop in intensity in the ionomer peak and an in increase in intensity of the crystalline long period peak, there are no other changes in the scattering profiles. Therefore, these data indicate no morphological changes occur within the sample at the β relaxation.

Given the persistent morphology at the β relaxation, it is reasonable to conclude that changes in SAXS peak intensities are due to specific variations in scattering contrast. Fischer and co-workers[68] have shown that the temperature dependence of the scattering intensity (I_{max}) of the long period peak for semicrystalline polymers can be expressed in the following equation

$$\sqrt{\frac{I_{max}(T)}{I_{max}(T_0)}} = 1 + \frac{(\alpha_a - \alpha_c)(T - T_0)}{\Delta\rho_0} \quad (5)$$

where α_a and α_c are the thermal expansion coefficients of the amorphous and crystalline phases, respectively, and $\Delta\rho_0$ is the density difference between the amorphous and crystalline phases at some reference temperature, T_0. According to eq 5, an abrupt change in α_a due to the glass transition will cause a change in the slope of the intensity−temperature curve. In agreement with this analysis, the data in Figure 15B show a significant change in the square root of the intensity, for the long period peak of TMA^+-form Nafion. This change in slope occurs over the temperature range from ca. 105 to 115 °C and coincides with the onset of the β relaxation. If one considers Nafion a three-phase system consisting of crystalline, amorphous, and ionic domains in order of decreasing density, then the relative change in density at the T_g can also explain the drop in intensity of the ionomer peak at the β relaxation. The scattering intensity is proportional to $(\Delta\rho)^2$, and as the density of the amorphous phase decreases, it is more closely matched to the density of the ionic domains, thus reducing the contrast (i.e., intensity). Conversely, the contrast increases between the amorphous and crystalline domains. From these data, it is now possible to assign the β relaxation to the genuine glass transition of Nafion. It should be clarified, however, that this is not simply a T_g of the matrix but is due to segmental motions (principally backbone motions on the length scale of 30−130 Å) within a *static* electrostatic network.

Conclusions

In this paper we have presented an explanation as to the molecular origins for the thermal events observed in the DSC and the mechanical relaxations observed in the DMA of perfluorosulfonate ionomers. From DSC studies, we conclude that the high-temperature endotherm observed is due to the melting of PTFE-like crystallites and not the T_g of the ionic domains as earlier suggested. Likewise, the low-temperature endotherm observed upon annealing, or simply drying at elevated temperatures, is due to the melting of small, imperfect crystallites that are formed in thermal equilibrium with the annealing (or drying) temperature. This annealing phenomenon is consistent with the crystallization behavior of a wide range of semicrystalline polymers, and thus the low-temperature endotherm is *not* attributed to the matrix T_g of Nafion or an order−disorder transition within the clusters.

The discussion of the molecular origins for the mechanical relaxations in Nafion has taken into consideration data obtained from DMA, variable temperature SAXS, and variable temperature solid-state ^{19}F NMR. Although a dual T_g explanation for two DMA relaxations, where the β relaxation is related to the T_g of the matrix and the α relaxation is related to the T_g of regions of restricted mobility, is acceptable for polystyrene- and polyethylene-based ionomers, it is an inaccurate description of the behavior with Nafion. By correlating the results from DMA with variable temperature SAXS and ^{19}F NMR, we have been able to link the α relaxation (DMA) to changes in the ionomer morphology of Nafion and molecular motions of both the side and main chains (^{19}F NMR). These data suggest that the α relaxation is due to the onset of long-range mobility of both the main and side chains facilitated by a profound weakening of the electrostatic interactions within the ionic aggregates. At temperatures in the vicinity of the α relaxation, a significant destabilization of the electrostatic network may be observed (i.e., through the activation of a *dynamic* network involving significant ion-hopping processes). In contrast, the β relaxation is associated with the onset of thermally activated main-chain motions that are facilitated through side-chain mobility within the framework of a *static* physical (electrostatic) network. Through this study, the β relaxation is now assigned to the genuine T_g of Nafion.

Acknowledgment. The authors acknowledge DuPont for providing the Nafion membranes. Support for this work was provided by DuPont, the NSF MRSEC program, NSF EPSCoR, and the American Society for Engineering Education, National Defense Science and Engineering Graduate Fellowship. SAXS data were collected at the National Synchrotron Light Source, Brookhaven National Laboratory, in collaboration with Dr. Forrest Landis at NIST (supported in part by the U.S. Department of Energy, Division of Materials Sciences and Divison of Chemical Sciences, under Contract DE-AC02-98CCCCH10886). Special thanks are also due to Dr. William Jarrett for his contributions in the area of solid-state ^{19}F NMR techniques and to Klaus Schmidt-Rohr at Iowa State University for many helpful discussions concerning the NMR data.

References and Notes

(1) Grot, W. *Chem.-Ing.-Tech.* **1978**, *50*, 299.
(2) Yeo, R. S.; McBreen, J.; Kissel, G.; Kulesa, F.; Srinivasan, S. *J. Appl. Electrochem.* **1980**, *10*, 741.
(3) Mauritz, K. A.; Moore, R. B. *Chem. Rev.* **2004**, *104*, 4535−4585.
(4) Doyle, M.; Rajendran, G. In *Handbook of Fuel Cells—Fundamentals, Technology, and Applications*; Vielstich, W., Lamm, A., Gasteiger, H. A., Eds.; John Wiley & Sons: New York, 2003; Vol. 3, pp 351−395.
(5) Gierke, T. D.; Munn, G. E.; Wilson, F. C. *J. Polym. Sci.,Polym. Phys. Ed.* **1981**, *19*, 1687−1704.
(6) Starkweather, H. W. *Macromolecules* **1982**, *15*, 320−323.
(7) Moore, R. B.; Martin, C. R. *Macromolecules* **1988**, *21*, 1334−1339.
(8) Fujimura, M.; Hashimoto, T.; Kawai, H. *Macromolecules* **1981**, *14*, 1309−1315.
(9) Fujimura, M.; Hashimoto, T.; Kawai, H. *Macromolecules* **1982**, *15*, 136−144.
(10) Gebel, G.; Lambard, J. *Macromolecules* **1997**, *30*, 7914−7920.
(11) Moore, R. B.; Martin, C. R. *Macromolecules* **1989**, *22*, 3594−3599.
(12) Roche, E. J.; Pineri, M.; Duplessix, R.; Levelut, A. M. *J. Polym. Sci., Polym. Phys. Ed.* **1981**, *19*, 1−11.
(13) Roche, E. J.; Pineri, M.; Duplessix, R. *J. Polym. Sci., Polym. Phys. Ed.* **1982**, *20*, 107−116.
(14) Elliot, J. A.; Hanna, S.; Elliot, A. M. S.; Cooley, G. E. *Macromolecules* **2000**, *33*, 4161−4171.
(15) Elliot, J. A.; James, P. J.; McMaster, T. J.; Newton, J. M.; Elliot, A. M. S.; Hanna, S.; Miles, M. J. *e-Polym.* **2001**.
(16) Gebel, G.; Aldebert, P.; Pineri, M. *Macromolecules* **1987**, *20*, 1425−1428.
(17) Gebel, G.; Moore, R. B. *Macromolecules* **2000**, *33*, 4850−4855.
(18) Rollet, A.-L.; Diat, O.; Gebel, G. *J. Phys. Chem. B* **2002**, *106*, 3033−3036.
(19) Rubatat, L.; Rollet, A. L.; Gebel, G.; Diat, O. *Macromolecules* **2002**, *35*, 4050−4055.
(20) Almeida, S. H. d.; Kawano, Y. *J. Therm. Anal. Calorim.* **1999**, *58*, 569−577.
(21) Hodge, I. M.; Eisenberg, A. *Macromolecules* **1978**, *11*, 289−293.
(22) Kyu, T.; Hashiyama, M.; Eisenberg, A. *Can. J. Chem.* **1983**, *61*, 680−687.
(23) Moore, R. B.; Cable, K. M.; Croley, T. L. *J. Membr. Sci.* **1992**, *75*, 7−14.

(24) Yeo, S. C.; Eisenberg, A. *J. Appl. Polym. Sci.* **1977**, *21*, 875−898.
(25) Nakano, Y.; MacKnight, W. J. *Macromolecules* **1984**, *17*, 1585−1591.
(26) Moore, R. B.; Cable, K. M. *Polym. Prepr.* **1997**, *38*, 272−273.
(27) Su, S.; Mauritz, K. A. *Macromolecules* **1994**, *27*, 2079−2086.
(28) Deng, Z. D.; Mauritz, K. A. *Macromolecules* **1992**, *25*, 2739−2745.
(29) Deng, Z. D.; Mauritz, K. A. *Macromolecules* **1992**, *25*, 2369−2380.
(30) Su, S.; Mauritz, K. A. *Polym. Prepr.* **1994**, *35*, 795−796.
(31) Miura, Y.; Yoshida, H. *Thermochim. Acta* **1990**, *163*, 161−168.
(32) Grot, W. G. E.J. du Pont de Nemours and Company, US 3,-718,627, 1973.
(33) Cable, K. M. Department of Polymer Science, The University of Southern Mississippi, Hattiesburg, 1996; p 170.
(34) Caravatti, P.; Bodenhausen, G.; Ernst, R. R. *J. Magn. Reson.* **1983**, *55*, 88−103.
(35) Cory, D. G.; Ritchey, W. M. *J. Magn. Reson.* **1988**, *80*, 128−132.
(36) Meresi, G.; Wang, Y.; Bandis, A.; Inglefield, P. T.; Jones, A. A.; Wen, W.-Y. *Polymer* **2001**, *42*, 6153−6160.
(37) Page, K. A.; Moore, R. B. *Polym. Prepr.* **2003**, *44* (1), 1144−1145.
(38) Orler, E. B.; Moore, R. B. *Macromolecules* **1994**, *27*, 4774−4779.
(39) Orler, E. B.; Calhoun, B. H.; Moore, R. B. *Macromolecules* **1996**, *29*, 5965−5971.
(40) Alizadeh, A.; Richardson, L.; Xu, J.; McCartney, S.; Marand, H.; Cheung, Y. W.; Chum, S. *Macromolecules* **1999**, *32*, 6221−6235.
(41) Kohzaki, M.; Tsujita, Y.; Takizawa, A.; Kinoshita, T. *J. Appl. Polym. Sci.* **1987**, *33*, 2393−2402.
(42) Lemstra, P. J.; Kooistra, T.; Challa, G. *J. Polym. Sci., Part A-2* **1972**, *10*, 823−833.
(43) Nichols, M. E.; Robertson, R. E. *J. Polym. Sci., Part B: Polym. Phys.* **1992**, *30*, 755−768.
(44) Tsujita, Y.; Shibayama, K.; Takizawa, A.; Kinoshita, T.; Uematsu, I. *J. Appl. Polym. Sci.* **1987**, *33*, 1307−1314.
(45) Cheng, S. Z. D.; Cao, M.-Y.; Wunderlich, B. *Macromolecules* **1986**, *19*, 1868−1876.
(46) Feldheim, D. L.; Lawson, D. R.; Martin, C. R. *J. Polym. Sci., Part B: Polym. Phys.* **1993**, *31*, 953−957.
(47) Weiss, R. A.; Agarwai, P. K.; Lundberg, R. D. *J. Appl. Polym. Sci.* **1984**, *29*, 2719−2734.
(48) Kim, J. S.; Yoshikawa, K.; Eisenberg, A. *Macromolecules* **1994**, *27*, 6347−6357.
(49) Hird, B.; Eisenberg, A. *Macromolecules* **1992**, *25*, 6466−6474.
(50) Chen, Q.; Schmidt-Rohr, K. *Macromolecules* **2004**, *37*, 5995−6003.
(51) Boyle, N. G.; McBrierty, V. J.; Eisenberg, A. *Macromolecules* **1983**, *16*, 80−84.
(52) Liu, S.-F.; Schmidt-Rohr, K. *Macromolecules* **2001**, *34*, 8416−8418.
(53) Schlick, S.; Gebel, G.; Pineri, M.; Volino, F. *Macromolecules* **1991**, *24*, 3517−3521.
(54) Slade, R. C. T.; Barker, J. *Solid State Ionics* **1989**, *35*, 11−15.
(55) Hietala, S.; Maunu, S. L.; Sundholm, F. *J. Polym. Sci., Part B: Polym. Phys.* **2000**, *38*, 3277−3284.
(56) Gong, X.; Bandis, A.; Tao, A.; Meresi, G.; Wang, Y.; Inglefield, P. T.; Jones, A. A.; Wen, W.-Y. *Polymer* **2001**, *42*, 6485−6492.
(57) MacMillan, B.; Sharp, A. R.; Armstrong, R. L. *Polymer* **1999**, *40*, 2481−2485.
(58) MacMillan, B.; Sharp, A. R.; Armstrong, R. L. *Polymer* **1999**, *40*, 2471−2480.
(59) Giotto, M. V.; Zhang, J.; Inglefield, P. T.; Wen, W.-Y.; Jones, A. A. *Macromolecules* **2003**, *36*, 4397−4403.
(60) Haryadi; Rankothge, M.; Hook, J.; Gorkom, L. v.; Moran, G. *Magn. Reson. Chem.* **1994**, *32*, 446−451.
(61) Rankothge, M.; Hook, J.; Moran, G. *Bull. Magn. Reson.* **1996**, *18*, 137−138.
(62) Rankothge, M.; Hook, J.; Gorkon, L. v.; Moran, G. *Macromolecules* **1997**, *30*, 4357−4362.
(63) Kang, H. W.; Moran, G. *J. Membr. Sci.* **1998**, *148*, 173−184.
(64) VanderHart, D. L.; McFadden, G. B. *Solid State Nucl. Magn. Reson.* **1996**, *7*, 45−66.
(65) Mehring, M. *Principles of High-Resolution NMR in Solids*, 2nd ed.; Springer-Verlag: Berlin, 1983.
(66) Kulbaba, K.; Manners, I.; Macdonald, P. M. *Macromolecules* **2002**, *35*, 10014−10025.
(67) Kim, J. S.; Roberts, S. B.; Eisenberg, A.; Moore, R. B. *Macromolecules* **1993**, *26*, 5256−5258.
(68) Fischer, E. W.; Kloos, F.; Lieser, G. *Polym. Lett.* **1969**, *7*, 845−850.

MA0503559